DTM generation from STC-SIMBIO-SYS images

C.Re [a] *, E. Simioni [a] , G.Cremonese [a], R.Roncella [b], G. Forlani [b], Vania Da Deppo[c] , G.Naletto[d], G.Salemi[e]

[a] INAF Astronomical Observatory, Padova, Italy, [b] Dept. of Civil Engineering, Parma University, Parma, Italy, [c] CNR-IFN Luxor, Padova, Italy, [d] Centro Interdipartimentale Studi e Attività Spaziali (CISAS) - G. Colombo, University of Padova, Padova Italy, [e] Department of Cultural Heritage: Archaeology and History of Art, Cinema and Music, University of Padova, Italy

ABSTRACT

The research group with the responsibility of the STereo Camera (STC) for the ESA BepiColombo mission to Mercury, has realized an innovative and compact camera design in which the light collected independently by two optical channels at ±20° with respect to the nadir direction converges on unique bidimensional detector. STC will provide the 3D-mapping of Mercury surface, acquiring images from two different perspectives. A stereo validation setup has been developed in order to give a much greater confidence to the novel instrument design and to get an on ground verification of the actual accuracies in obtaining elevation information from stereo pairs. A series of stereo-pairs of an anorthosite stone sample (good analogue of the hermean surface) and of a modelled piece of concrete, acquired in calibration clean room by means of an auxiliary optical system, have been processed in the photogrammetric pipeline using image correlation for the 3D model generation. The stereo reconstruction validation has been performed by comparing the STC DTMs (Digital Terrain Models) to an high resolution laser scanning 3D model of the stone samples as reference data. The latter has a much higher precision (ca. 20 μm) of the expected in-lab STC DTM (190 μm). Processing parameters have been varied in order to test their influence on the DTM generation accuracy. The main aim is to define the best illumination conditions and the process settings in order to obtain the best DTMs in terms of accuracy and completeness, seeking the best match between the mission constraints and the specific matching aspects that could affect the mapping process.

Keywords: Planetary Mapping, Stereo Reconstruction, DTM, Reconstruction Accuracy, Area Based Image Matching

1. STC STEREO VALIDATION CONCEPT

1.1 Motivations and Objectives

In 2017 two different orbiters (ESA Mercury Planetary Orbiter, MPO, and JAXA Mercury Magnetospheric Orbiter, MMO) will be launched from Kourou to the innermost planet of the Solar System, Mercury. Scope of this mission, called BepiColombo, is the study to characterize the planet Mercury, being the end-member of the Solar System, and to improve the knowledge of some important constants of fundamental physics.

Onboard the satellite the SIMBIO–SYS package (Figure 1(a)) integrates on a common optical bench instruments with different functions and operating on different channels . SIMBIO–SYS will provide a global view of Mercury and local high resolution images in order to reconstruct the overall evolution of the planet. The suite includes two imaging systems respectively with stereo (STC) and high spatial resolution (HRIC) capabilities and a hyperspectral imager (VIHI) in the visible-near infrared range. STC is based on an innovative compact design characterized by two separated optical channels inclined to form a stereo angle of 40°. The two channels share the majority of the optical elements and the bidimensional detector.

The design in based on a single focal plane assembly for both the sub-channels, while common stereo systems usually consist of two identical cameras, each with its own detector. This solution combines good stereo performance and at the

*cristina.re@oapd.inaf.it

Videometrics, Range Imaging, and Applications XIII, edited by Fabio Remondino, Mark R. Shortis,
Proc. of SPIE Vol. 9528, 95280P · © 2015 SPIE · CCC code: 0277-786X/15/$18 · doi: 10.1117/12.2184745

same time, being very compact, savings in mass and volume: from the optical point of view lens design reduces the telescope length by about a factor 2 with respect to the classical configuration. The common telescope unit and the unique CMOS hybrid detector complete the brand new design.

In order to verify the actual capability on the new system, an innovative setup has been conceived and realized. With this setup, the STC acquisition process has been scaled-down at the laboratory scale, applying the photogrammetric 3D surface reconstruction to known targets.

The calibration procedures are more complex than for other standard space cameras. The process is finalized, not only in the estimation of the standard intrinsic parameters (the focal length , distortion parameters, principal point position…) for both channels, but also the extrinsic parameters between the two channels. It is also fundamental to verify the instrument capability to reconstruct the surface of the planet with a desired accuracy.

The accuracy of the 3D reconstruction depends on the accuracy of the knowledge of intrinsic and extrinsic parameters of the optical system and the accuracy of the image matching procedure (i.e. image coordinates precision). The interior orientation parameters estimation has been retrieved by the calibration campaign data. The geometrical tests, by means of physical and optical measurements allowed to determine the focal length and the principal point position for both the channels despite the off-axis configuration. The determination of the extrinsic parameters has been quite difficult for the long focal length, very small sensor size, narrow FoV (Field of View), etc. Two different algorithmic approaches have been considered to provide the orientation solution: Bundle block adjustment with ground control points (GCP), an established photogrammetric procedure, and Zhang's [1] algorithm.

To verify the 3D reconstruction capabilities of STC Flight Model (FM), the sample targets have been measured with a very accurate 3D laser scanner in order to have a known reference surface with an accuracy higher than the expected photogrammetric one. The comparison between the height information retrieved from stereo reconstruction and the laser scanner has allowed an evaluation of the stereo system's performance both in terms of horizontal resolution and vertical accuracy [2]. Those indexes can be used to evaluate both the quality of the designed stereo camera and the goodness of the implemented stereo validation method; the latter allowing for the first time to test in laboratory the stereo capability of a flight instrument.

a)

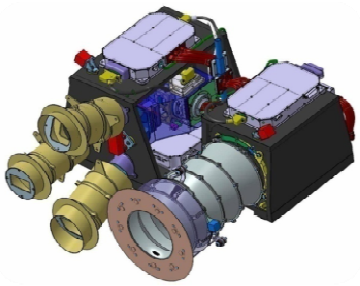

b)

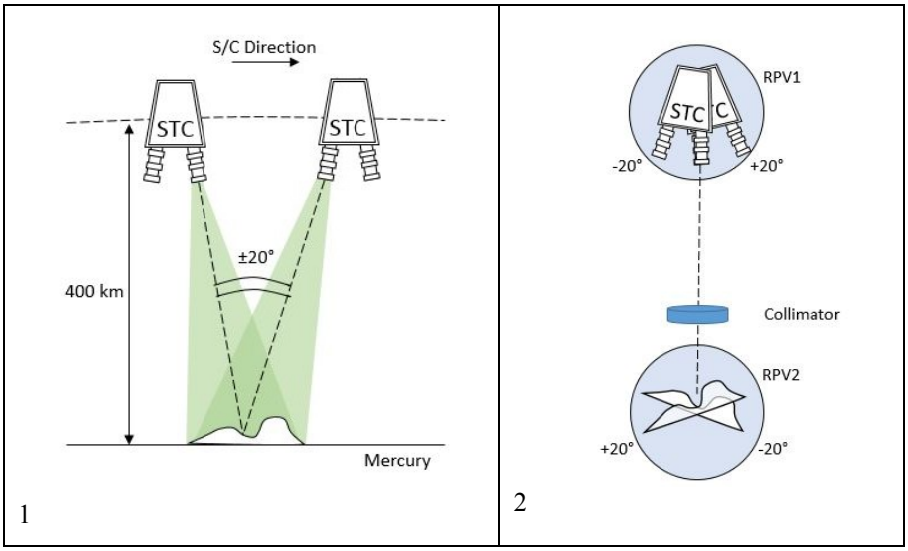

Figure 1. (a) SIMBIO-SYS instruments suite layout. (b) Setup for STC stereo validation concept design: 1. STC flight observing conditions at periherm. 2. In laboratory simulation of STC observing with "Forward channel" (F) and "Backward channel" (B) at periherm by means of the stereo validation setup. STC FM and target rotations are provided by high precision motorized rotation stages (RPV).

1.2 The Stereo Validation Setup (SVS): optical and mechanical design

In order to estimate and characterize the actual stereo reconstruction capabilities of STC, an indoor Stereo Validation Setup (SVS) has been developed.

Since in-flight STC will acquire images of the Mercury surface from more than 400 km distance with several hundred km baselenghts, an auxiliary optical system, that allows the indoor acquisition of images, is needed to test the instrument. The concept adopted is that a target projected at infinity by a 1-m focal length collimator, can be considered as a representation of the Mercury surface at 400 km distance (Fig. 1 (b.1)).

The SVS is a combination of optical and mechanical components that allows the indoor reproduction of the instrument observing conditions: the same object area is imaged first by the Forward looking channel and, in a second moment, by the Backward looking channel. The indoor simulation of the spacecraft trajectory (for simplicity only the periherm is considered) is provided by two rotation stages (Fig. 1 (b.2)).

The main components of the stereo validation setup (see Figure 2 (a)) are:

- the collimator lens (achromatic doublet with focal length of 1000 mm with a diameter of 80 mm)

- a motorized rotation stage which simulates the stereo angle of STC (RPV)

- a target positioned on the RPV rotation stage,

- a light source

Everything is mounted over an optical breadboard to facilitate the integration with the optical ground support equipment (OGSE).

A reference cube is positioned over the rotation axis of the target plate for the pre-calibration alignment activities. The first rotation stage, where the STC instrument is positioned, has the function of aligning the optical axis of the active STC channel with the collimated light coming from the collimator lens; the second rotation stage has the function of rotating a target positioned on the collimator lens focusing point, reproducing the angle between a pair of homologous rays [2].

STC SVS light source (narrow-spot halogen lamp) has been mounted over a curve rail system conceived to rotate together with the target support plate maintaining a constant lighting condition. The support has been designed providing the same light incidence angle for both left and right (or forward and backward) images of stereo couples to reproduce some of the possible light incidence angles (10°, 30°, 50° and 70°) referring to the possible Sun rays incidence angles to the Mercury surface when the spacecraft is at periherm.

The vertical accuracy requirement in SVS case has been computed by preserving the ratio between the horizontal resolution and vertical accuracy requirements of STC at periherm. At periherm the observing distance is about 400 km with a pixel scale on ground of ca. 50 m. To obtain the same (scaled) spatial resolution with a 1 meter collimator focal length the target surface should be sampled with a step of 105 μm and the elevation should be determined with an accuracy of 190 μm.

A summary of the principal stereo reconstruction parameters for STC stereo design and its indoor dual model is shown in the following Table:

Parameter	STC	SVS
f (mm)	95 mm	~170 mm
Pixel size (μm)	10 μm	10 μm
FoV (deg)	5.3°×2.4°	3°×1.36°
Target distance	400 km	~1600 mm
Target Footprint	37×17 km^2	92×42 mm^2
Ground Sampling Distance (GSD)	50 m/pix	~105 μm/pix
Vertical Accuracy	~80 m	~190 μm

Table 1. Stereo reconstruction design parameter in the real periherm case and in dual SVS.

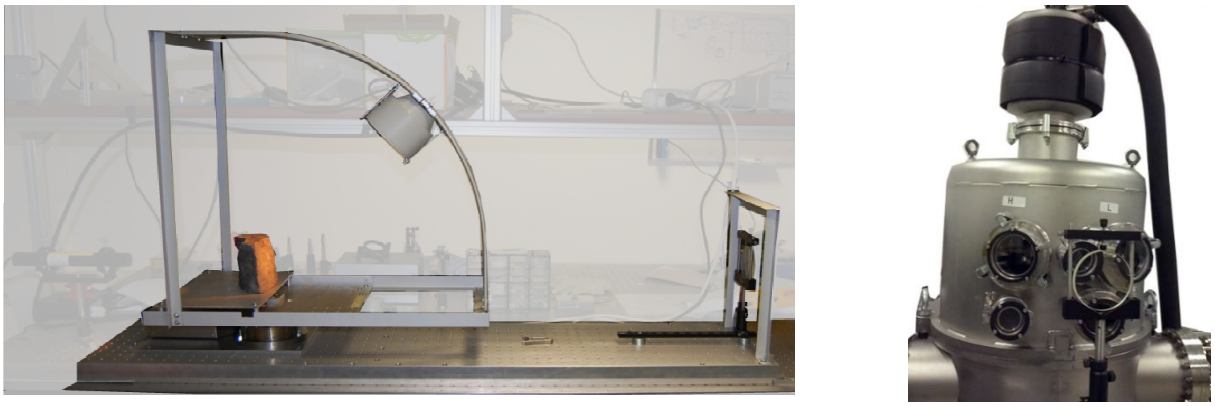

(a) (b)

Figure 2. (a) The SVS. The halogen lamp is mounted on the first rotational stage where the target sample is positioned. A collimator (on the right side) completes the optical system permitting the use of STC indoor. (b) STC thermo-vacuum camera with the two different optical channels.

1.3 **Photogrammetric process**

The pipeline for DTM generation can be summarized as follows:

• Calibration of the optical channels

• Image orientation

• Point cloud (DTM) generation by dense image matching

The two optical channels of the instrument, aligned one by one with the collimator lens of the SVS, have been calibrated separately, each one by the combination of both the single optical channel and the collimator (1000 mm focal length) with a distance between these two elements of at least 1000 mm.

This optical design is characterized by an extremely long focal length and a very narrow field of view that has made the estimation of the exterior orientation parameters (by bundle block adjustment) very difficult. As according to [3] one of the practical impediments to the adoption of long focal length cameras in close-range photogrammetry is the difficulty in network exterior orientation and self-calibration that can be encountered with the collinearity equation model when the camera field of view is smaller than around 10°. As focal length increases, so the field of view becomes narrower. This can impact adversely on the collinearity equation model, since the bundle of rays can approach, in effect, a parallel projection.

The strong correlations between the perspective centre coordinates (X0, Y0, Z0) and the focal lengths are extremely high and different solutions for the focal length can be achieved with the same value of the standard error σ_0 indicating the impossibility to identify the right and stable system solution.

The principal point position of each camera has been obtained optically. At the moment, since considering the complexity of STC optical design, the distortion map is not describable in the classical radial and tangential components, an ad hoc model is still in development and for the tests the corresponding parameters have been neglected (the maximal evaluated distortion on the border of the filters is 0.5 pixel). At last, the focal lengths have been estimated by the Zhang's algorithm [1]. For this calibration, a suitable sized chessboard has been positioned on the object plane of the cameras and several images have been acquired varying its position and orientation. Then, from the analysis of these images, the focal

length estimation has been performed. Image orientation of the stereo pair (the determination of the extrinsic parameters) has been performed both by the stereo extension of the calibration rig approach through the Camera Calibration Toolbox (which provides an implementation of the Zhang's algorithm) and by a bundle block adjustment with tie and GCP (Ground Control Points).

1.3.1 Camera calibration and image orientation with Zhang algorithm

The calibration process by Zhang algorithm is based on the detection of chessboard corners (or feature detection) implemented with standard edge detection algorithm [1] a set of images of the calibration target in different positions provides sufficient information to compute a robust estimation of camera parameters. Since the corner coordinates extraction process is affected by error, the calibration algorithm computes a maximum likelihood estimation of camera parameters which minimize the overall back-projection error.

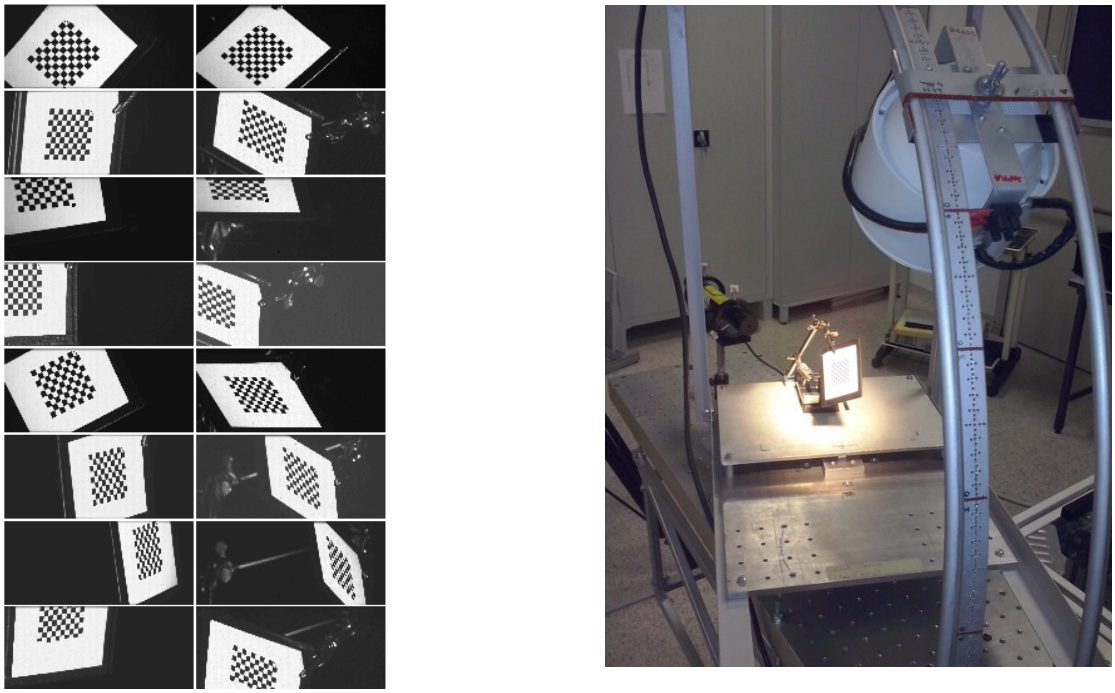

(a) (b)

Figure 3**.** (a) a subset of the images used for Zhang calibration. On the left the calibration chessboard acquired from the backward panchromatic filter; on the right those acquired by the forward one (right side). (b) the chessboard (3 mm for chess) used during STC calibration.

For each image of the calibration target an homography matrix is computed through a maximum likelihood estimation (performed with the Levenberg-Marquard algorithm [4]). The homographies are then combined together to extract the values of intrinsic parameters. The calibration procedure described can be easily extended to the estimation of the extrinsic parameters of a stereo imaging system. If the calibration target is acquired simultaneously by the two cameras, the single camera calibration data can be easily combined to get information about the mutual position of the two cameras and the effective position of the calibration chessboard in a common reference system (see Figure 3).

In the STC case the principal points for the two panchromatic filters were measured optically. The focal length was accurately estimated only for the telescope optical path without considering the collimator. Zhang's procedure was therefore applied fixing the boresights and estimating the focal lenses of the imaging system. The estimation of the extrinsic parameters produce a stereo angle of 42.27°.

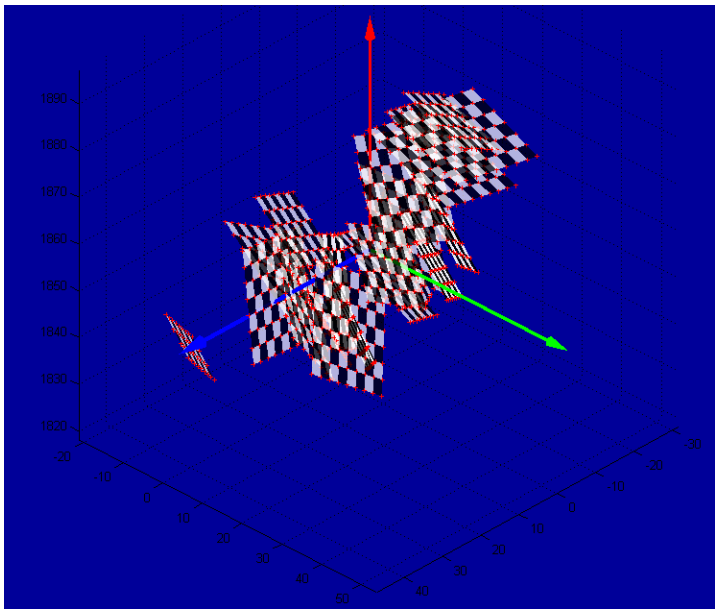

Figure 4**.** The reconstruction of the chessboard in different orientations and position from Zhang's algorithm

The numerical instability of the system led to recompute the results by fixing different values of focal length demonstrating the independence of the stereo angle result from this parameter. The variability of the focal length imposed affects the baseline length and the target distance (which balance themselves) but preserve the angular geometry of the system.
Residual of the corners extracted from chessboard images are shown in Figure 5.

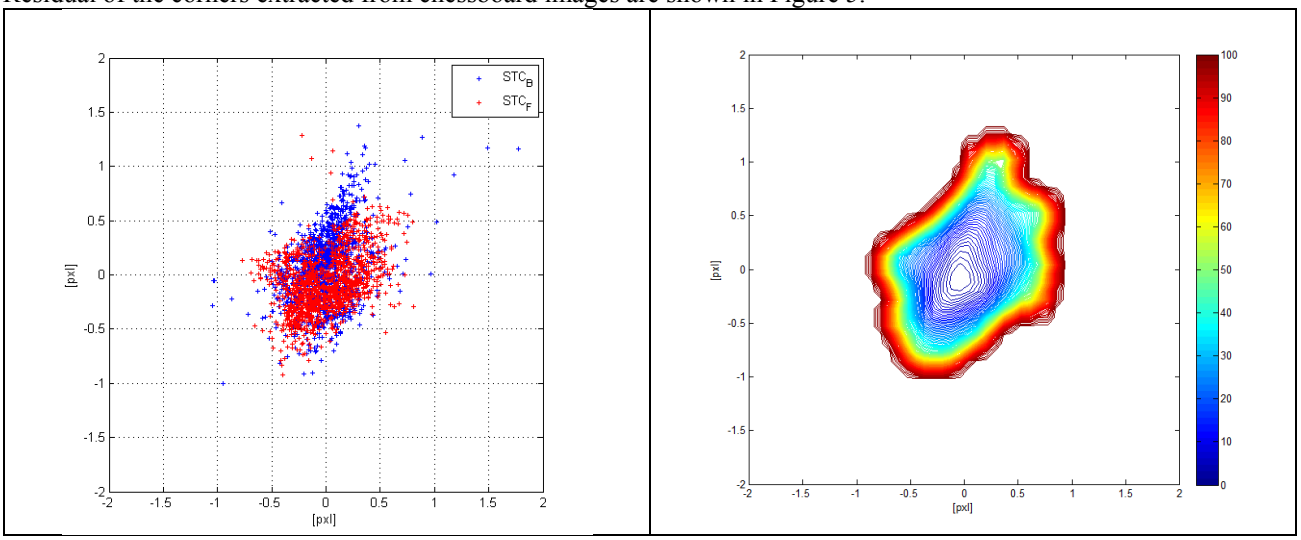

(a) (b)

Figure 5**.** Residuals at the chessboard corners (a) both for Forward and Backward channels and in (b) Isolines show the percentile distribution of the residual..

1.3.2 Image orientantion by Bundle adjustment with Ground Control Points (GCP)

A bundle adjustment has been performed with the program Photomodeler, the commercial software by Eos Systems Inc; a set of extracted image points have been imported and have been superimposed on the images; the object coordinates of the GCPs have been imported and associated by manual collimation in both images; the camera interior parameters from optical calibration have been set manually in the camera properties mask. Due to their role in the bundle adjustment procedure, the identification and accurate measurement of the image coordinates of the GCP is very important. According to the accuracy and density of laser scanning data, any point in the reference DTM can in principle be selected as GCP; in practice, a matching between the image of the point and its location in the DTM is necessary in order to measure image and object coordinates; the visual identification of the feature in both the image and the DTM is therefore required. Since the FARO laser system (see Section 3) used to provide the reference data does not deliver color information, the accuracy of the identification (of an image point on the DTM or of a DTM feature on the image) was not very accurate in the initial tests and required a great deal of effort to reach a good result. To improve the accuracy of this matching, in successive tests pins have been attached to the rock samples (see Figure 6) to allow an easy, accurate and non-ambiguous identification of GCP's both in the images and in the reference DTM.

2. DTM GENERATION

2.1 Dense Matching Implementation

The DTM generation has been carried out by the Dense Matcher program (DM) [5]. The software, written in C#, implements the NCC (Normalized Cross Correlation (Lewis, 1995) method, the Least Squares Matching (LSM) method [6] and the Multiphoto Geometrically Constrained Matching (MGCM) method [7]. The DM workflow for the DTM generation starts from a number of seed (tie) points generally extracted by SURF operator [8]. Through the Delaunay triangulation and the consequent interpolation, the starting location of the corresponding points on the slave image are determined and an approximate parallax field is defined. In providing initial parameters to the least squares estimate, in order to allow a coarse-to-fine multi-resolution algorithm implementation, a hierarchical approach has been used. For each level of the pyramid, the parallax values are interpolated on a grid and initial search of the correspondences through NCC algorithm is performed. At this point the disparity map is refined by the LSM. At the end of the image matching procedure all the correspondences are triangulated giving the 3D position of the object point.

An innovative LSM algorithm has been implemented to model the geometric transformation in image resampling using different shape functions as proposed by Bethmann [9]. The extended shape functions that have been applied for the tests beyond the common Affine transformation (6 parameters) are the Projective (8 param.) and the Polynomial (12 param.) transformations. These functions should improve details in shape reconstruction particularly where the object cannot be considered flat within the template.

2.2 Process configurations

The object point precision and accuracy in a photogrammetric DTM depends on several factors: viewing conditions (image geometry and illumination), errors affecting the calibration (determination of the intrinsic parameters), image orientation (determination of extrinsic parameters) and image measurements (matching capabilities).

The SVS gives the important opportunity to investigate some of these aspects and study their effect on surface reconstruction. The geometry of the stereo system composed by the two STC optical channels imaging the same portion of planet's surface depends on the latitude of the observed area, due to the eccentricity of the SC orbit. Considering the mean orbital parameters of the MPO over the nominal mission lifetime, the angles of incidence of the two optical channels and the stereo baselines have been computed as a function of the latitude observed at Mercury's surface. In addition to this mission constraint, the influence of the illumination conditions must be analysed in order to plan image acquisition but also in order to highlight problems with stereo pairs composed by images acquired at different times (in this case the presence of shadows become critical). The influence of the image orientation in the reconstruction is also crucial and both approaches (Bundle block adjustment by GCP and a calibration rig approach through Zhang algorithm)

have been performed and compared to check the consistency of the results. Three different shape models were applied in the LSM method to highlight differences in reconstruction accuracy.

The evaluation of the different process configurations has been carried out in terms of accuracy quantified by the RMS (Root Mean Square) error of the discrepancies between the DTMs generated by the stereo process and the laser reference acquisition and in terms of number of reconstructed points.

2.2.1 Illumination

The planned mission scenario will involve some specific photogrammetric requirements that need to be considered in the data exploitation. The illumination conditions and the block geometry are very important for the image processing success. The variability of the illumination in the datasets is an important factor to be analyzed in order to reach higher levels of accuracy and reliability in the reconstruction (particularly problematic for complex/irregular shapes). In order to evaluate this influence, the illumination setup has been conceived for this kind of investigation. In particular the lamp holder, thanks to a curve rail system, allows the setting of different light incidence angles, i.e. several observing conditions (see Figure 6)

A set of images for both the stones under four different incidence angles have been used for the generation of several DTMs.

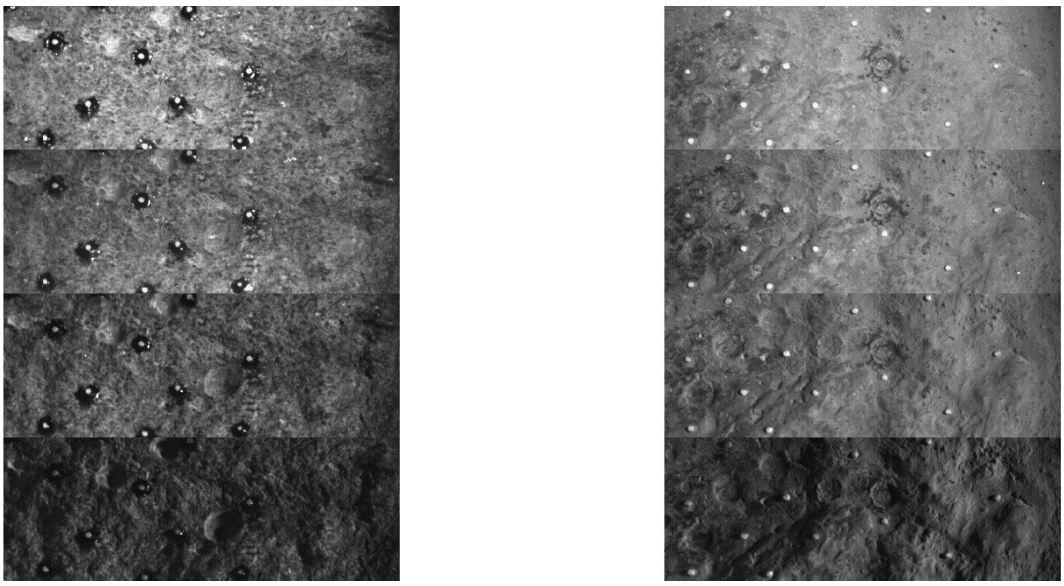

(a) (b)

Figure 6. The images show the effect of the four different illumination conditions on the image both for Anorthosite (a) and Concrete (b) samples.

It was found that higher contrast made easier the identification of features in the Structure from Motion (SFM) phase [10], producing a higher number of points (the so-called seed points of the dense matching) and this would be consistent also with [11], who found that at high illumination angles (with respect to the surface normal) the image entropy is maximised, based on a measure of image compressibility.

An useful tool for contrast enhancement is the image histogram. The image histogram describes the statistical distribution of image pixels in terms of number of pixels at each DN but it doesn't contains any information about spatial distribution of those pixels. Another statistical analysis was computed: the color maps on the left side in Figure 7 show the distribution of local DN standard deviation (σ) on the master image evaluated on a window of (19x19 pixel). In

the case of concrete, analyzing the histograms of the local σ and the color maps we note that images acquired at high lighting angles with respect to the surface normal (50/70 deg) show higher mean values, which would improve the accuracy of the matching algorithms.

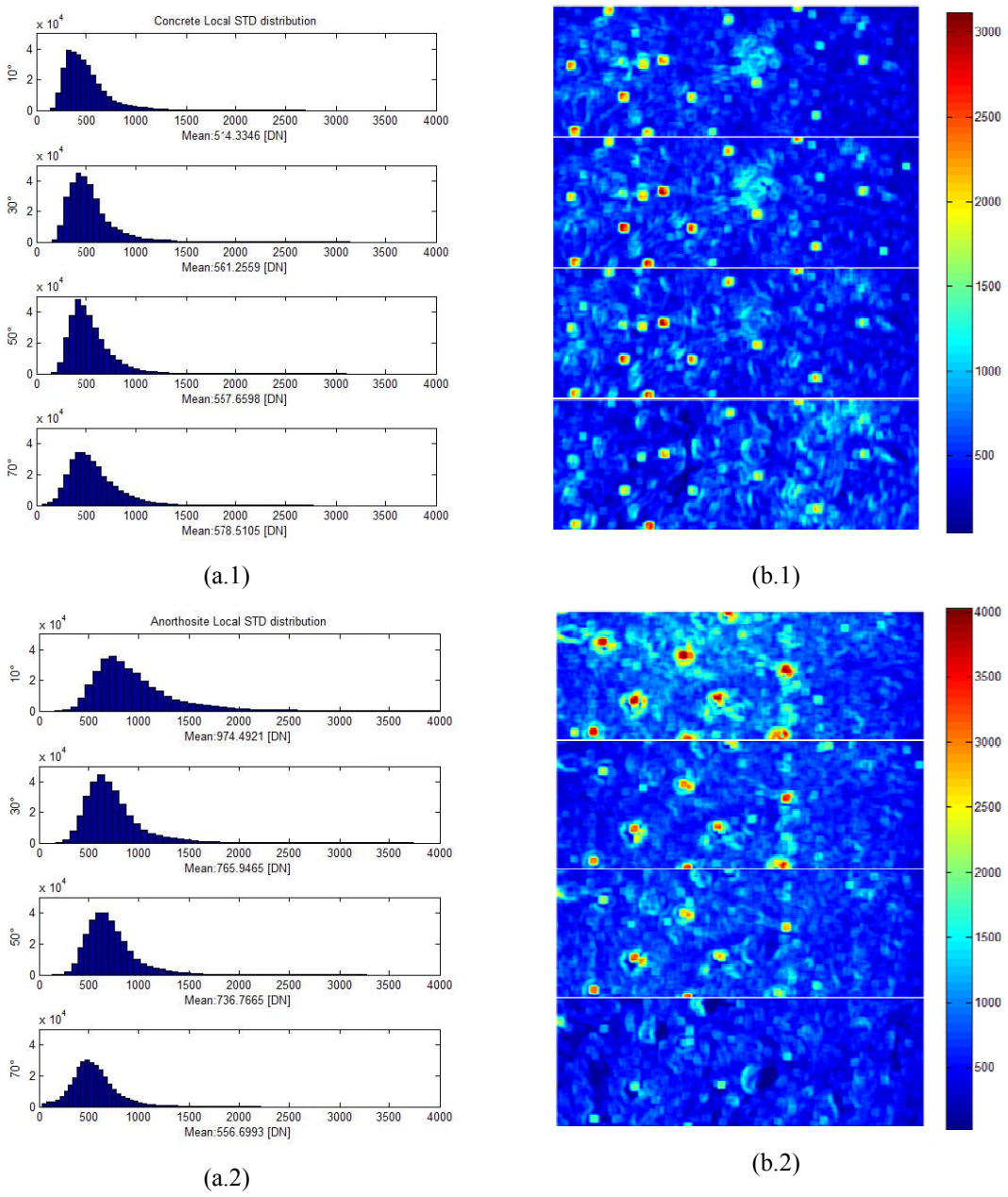

Figure 7. Figure shows the local std analysis both for Anorthosite sample (1) and Concrete (2) one. In (a) the histograms of the local std at different illumination angles are shown. In (b) the colour map of the local std shown for the master images. Color bars are expressed in DN.

The Anorthosite case is quite difficult and controversial in the interpretation because, as seen in the Figure 3(a), the glue used to attach the pins reflects the light, then the stone has tiny crystals making the surface reflective and creating some saturated points, clearly visible also in the color map of the local std. The presence of spot reflections could be problematic as could be the shadows created by complex surfaces (in both cases large differences in the images may cause gross matching failures).

3. LASER SCANNER ACQUISITION

In order to check the consistency of the stereo reconstruction, the stereo DTM produced by Dense Matcher has to be compared with a reference DTM of the rock samples. The latter has been provided by a CAM2® FaroArm Platinum scanner system, a portable Coordinate Measurement Machine (CMM) with a Z axis accuracy of 0.02 mm collected in the form of a point clouds convertible in a mesh of equidistant points on a XY grid. The grid spacing of the laser scanner was actually rather poor (400 μm) with respect to our needs. However, the limit was circumvented by repeated scans. In this way, many more points are measured on the target surface, and it has been possible to reconstruct a much denser grid down to the required resolution using a suitable interpolation of the data. The reference surface (Figure 8) has been produced by interpolation on a grid with point spacing of 0.05 mm (about half of the image resolution).

a) b)

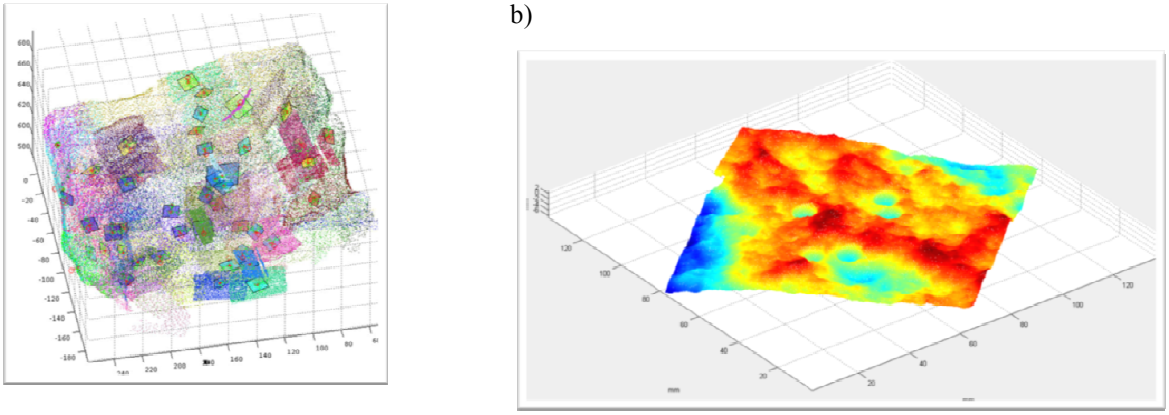

Figure 8. a) Many scans of the rock surface are reported with different colors, b) The laser scan interpolated 3d surface

4. STEREO VALIDATION

4.1 COMPARISONS AND ACCURACY EVALUATION

The comparison between the stereo products and the reference gave the confidence about the capability of the system to perform stereoscopic imaging, and allowed to estimate the performance of the Dense Matcher software in this specific application with different processing parameters. The comparison has been performed by importing both point clouds (the reference one and the one generated by Dense Matcher) in a 3D modeling software where several tools are available; in particular, the point cloud can be interpolated to generate a surface; point clouds or surfaces can be co-registered keeping one fixed and rigidly adapting the other with the ICP (Iterative Closest Point) algorithm [12]. The algorithm iteratively estimates the transformation (combination of translation and rotation) needed to minimize the distance from the source to the reference point cloud.

The settings for the comparison allow to exclude from the ICP registration points that are too far from the surface (such as gross errors in the data). In particular a threshold of 0.5 mm has been considered adequate since with this value the 99 % (assuming a normal distribution of the errors) of the points is included within 4 (σ).Once the iterations of ICP are completed, the signed or the absolute distance of each point in the generated DTM from the reference surface can be computed and the relevant statistics are calculated; points that are located farther than a given threshold from the reference surface can be excluded from the statistics. In addition, a color error map is produced, where areas with points excluded from the comparison are left blank and the other are color-coded. If GCPs have been used, the obtained DTM is nominally already registered in the same system as the reference DTM, so no ICP iteration is in principle necessary; in

practice, as far as the validation of the object shape reconstruction is concerned, using ICP removes some effects caused by systematic errors in interior and exterior orientation parameters.

4.2 DTM ACCURACY EVALUATION: RESULTS

As far as the accuracy of reconstruction is concerned, the results have been organized considering the different process configurations in the DTM generation.

We have varied:

-the illumination angle in the image acquisition;

-the different approaches used to estimate the exterior orientation parameters

-the shape models in the LSM.

The following Figure shows the trends of the RMS error and of the number of good points varying the illumination angle and the shape function applied in the LSM for both the stones and the Tables show the results also considering the different approaches used in the estimation of the exterior parameters.

Concrete:

(a)

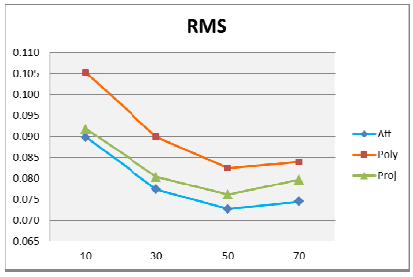

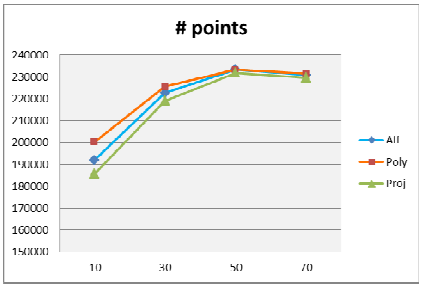

(b)

	Zhang		GCP	
	RMS (mm)	# pts	RMS (mm)	# pts
10°	0.079	187460	0.089	191908
30°	0.067	216463	0.077	222656
50°	0.063	226954	0.072	233394
70°	0.065	224523	0.074	230877

Anorthosite:

(c)

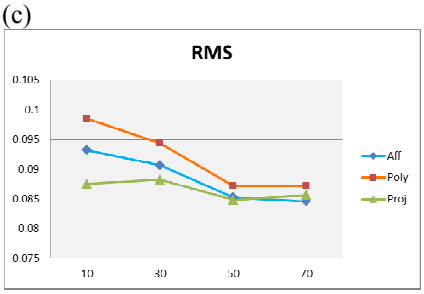

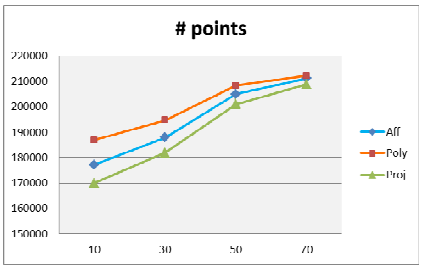

(d)

	Zhang		GCP	
	RMS (mm)	# pts	RMS (mm)	# pts
10°	0.093	171972	0.093	177218
30°	0.089	182110	0.090	187881
50°	0.084	198775	0.085	204967
70°	0.083	204620	0.084	211135

Figure 9: a) Concrete sample: RMS error and number of good points for the illumination angle increasing from 10° to 70° and different shape functions considering the Zhang method for the definition of the exterior parameters , b) results obtained with the Affine transformation and a template size of 19x19 pixel (RMS and number of points) for both the exterior orientation parameters estimation approaches and varying the illumination angle. (c) and (d) are related to the Anorthosite case.

Our results confirm the statement expressed in the paragraph 2.2.1 showing that the least-squares matching algorithms provide higher precision with images taken at higher illumination angles. What is evident from the trend of the graphs is that there is an increment in the accuracy and in the completeness of the models increasing the illumination angle. In particular the best result in terms of accuracy is reached for 50° of illumination angle (0.063 mm) for the concrete sample and at 70° of illumination (0.083 mm) for the anorthosite. Concerning the completeness, the number of good points is again maximum when the illumination angle is 50° for concrete (233394) and at 70° for the anorthosite with 211135. Those values are the best obtained considering both the bundle adjustment and the Zhang approach. From

Tables (b) and (c) in Figure 9 it appears that the approaches applied in the estimation of the exterior orientation parameters do not provide so different results: the Zhang method provides DTM that reach better RMS values from the comparison with the laser acquisition but the GCP solution appears to help in the generation of DTM more complete (233394 points is the max number of reconstructed points for the GCP solution versus 224523 for the Zhang application case).

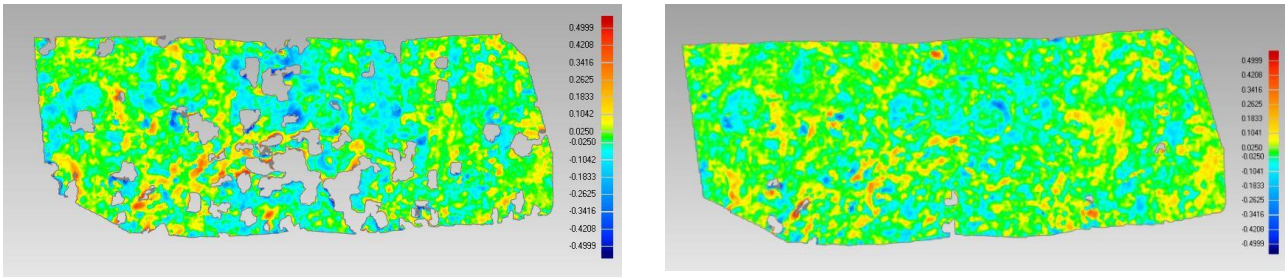

(a) (b)

Figure 10. Concrete color coded error map of the 3D reconstruction for 10 deg (a) and 50 deg (b) illumination angle

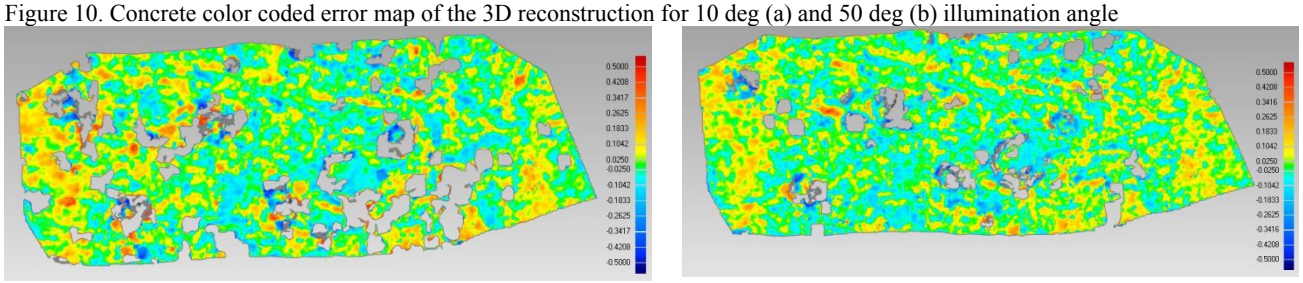

(a) (b)

Figure 11. Anorthosite color coded error map of the 3D reconstruction for 10 deg (a) and 50 deg (b) illumination angle

Looking at the color error maps (Figure 10 and 11), especially for the concrete sample, what is clearly visible is the completeness of the 50° acquired images with respect to the 10°. The color error maps suggest that the higher errors in sign occur where the surface roughness is higher and by a comparison with the images, the higher spikes are in correspondence with points of high reflectivity. In order to evaluate the influence of different illumination conditions for the images of the stereo-pair, a DTM has been generated from an image acquired with an illumination angle of 30°and another with 70°.
From the comparison with the reference model the results retrieved (RMS: 0.120 mm and 124624 good points) showed that the image correlator has difficulties in the matching process caused by the radiometric differences in the changing of illumination.

As far as the use of the alternative shape function in the LSM implementation is concerned, the fact that the polynomial transformation improves the capability to extract more details from the shape is quite clear looking at the model as in the Figure 12 but not so evident from the numerical results (Figure 9 (a) and (c)).
What is important to stress is that that the laser point cloud has higher precision and accuracy in elevation but a spatial resolution (point cloud density) lower than the photogrammetric models. Therefore we are somehow comparing the stereo-DTMs with a smoothed version of the rock surface (by laser) that is not basically able to highlight the potential of the more complex shape function (projective and polynomial) to model the surface in a finer way.

Affine (a)	Projective (b)
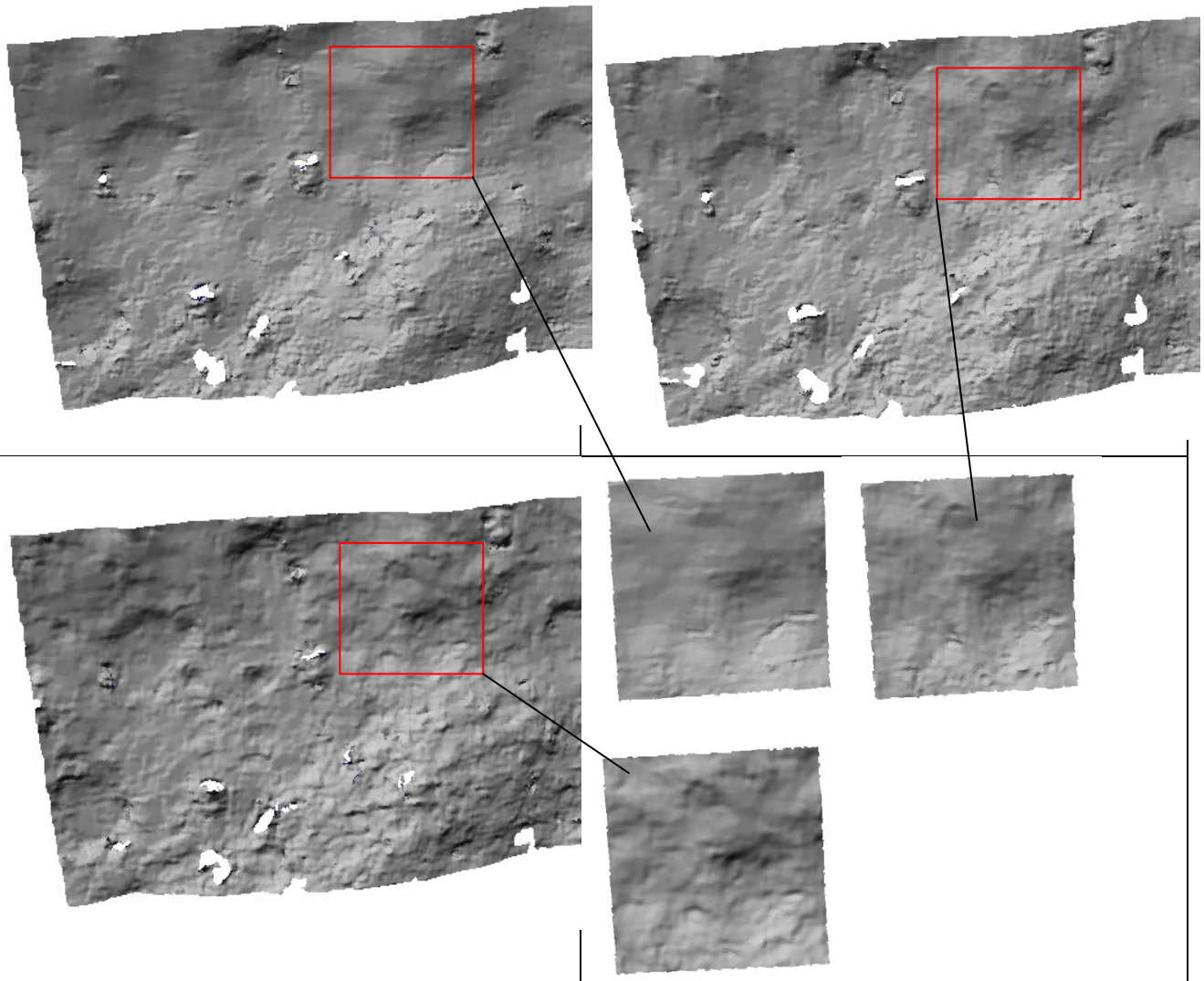	
Polynomial (c)	(d)

Figure 12: a) the DTM generated by the Affine shape model, b) the DTM generated by the Projective shape model, the DTM generated by the Polynomial shape model; d) the enlarged views clearly show the capability of the more complex shape models to capture surface details

5. CONCLUSIONS

An innovative setup for the validation of stereo reconstruction capabilities of the SIMBIO-SYS STC has been developed and tested with the flight model. The tests performed have been aimed to evaluate the impact of different sample morphologies and lighting conditions on stereo performance and on the other side to define the best process settings for the 3D reconstruction on real data.

The obtained RMS values are all well below the 190 micrometers that represent the requirement for STC at the breadboard scale (the best results obtained in the tests are 63 micrometers and the worst 93 micrometers). Also the number of reconstructed points varies considerably: the main reasons for such a variability are the characteristics of the rock sample surface that results in poor image texture and/or reflection spikes.
The importance of adequate illumination conditions within a set of stereo images after this investigation has been demonstrated to be relevant in the DTM generation both in terms of accuracy and completeness. The best configuration appears to be that one considering high angle of illumination from the nadir (oblique). This case shows that the correlator improves the matching success. Oblique illuminations cause large shadows in rough terrain, on the other hand, as in this study case where the altitude range (of the samples reported at the Mercury scale) is around 2500 m, the increasing contrast with higher angles seems to be a positive aspect in the 3D reconstruction. The matching strategies applied do not suggest yet clear results for the definition of the best shape model to be applied in the LSM. The choice of the transformation model is connected to the complexity of the surface and the use of higher order geometrical models can outperform efficiently the affine transformation especially in the case of smooth curved surfaces[13]. From this analysis the use of the Affine transformation provide overall the best results.
The comparison between the stereo products and the reference shows the capability of the system to perform stereoscopic imaging, and allowed to assess the performance of the Dense Matcher software in this specific application with the changing of different processing parameters.

REFERENCES

[1] Zhengyou Zhang, “Flexible - Camera Calibration By Viewing a Plane From Unknown Orientations”, International Conference on Computer Vision - ICCV , pp. 666-673, 1999, DOI: 10.1109/ICCV.1999.791289
[2] Naletto, G., Cesaro, M., Albasini, A., Cremonese, G., Da Deppo, V., Forlan,i G., Re, C., Roncella, R., Salemi G., Simioni E., “Innovative optical setup for testing a stereo camera for space applications”, Proc. SPIE 8442, Space Telescopes and Instrumentation, 2012
[3] Stamatopoulos, C., Fraser, C., & Cronk, S., “On the self-calibration of long focal length lenses”, International Archives of Photogrammetry, Remote Sensing and Spatial Information Sciences,Vol. XXXVIII, Part 5, 2010
[4] J. More. “The Levenberg-Marquardt algorithm, implementation and theory”, In: G. A. Watson, editor, Numerical Analysis, Lecture Notes in Mathematics, 630 pp. Springer Verlag, 1977.
[5] Re C., Roncella R., Forlani G., Cremonese G., Naletto G., “Evaluation of area-based image matching applied to DTM generation with Hirise images”, International Archives of Photogrammetry, Remote Sensing and Spatial Information Sciences, Vol XXXIX, Part IV/7, 2012
[6] Gruen, A.,”Adaptive least squares correlations: a powerful matching technique”, South African J. Photogramm. Remote Sensing and Cartography, 14(3), pp. 175-187, 1985.
[7] Gruen A and Baltsavias EP, “Geometrically Constrained Multiphoto Matching”, Photogrammetric. Engineering & Remote Sensing, 54(5), pp. 633-641, 1988.
[8] Bay, H., Ess, A., Tuytelaars, T., Van Gool, L., “SURF: Speeded up robust features”, CVIU, 110(3): 346-359, (2008).
[9] Bethmann, F., Luhmann,T., “Least-squares matching with advanced geometric transformation models”, International Archives of Photogrammetry, Remote Sensing and Spatial Information Sciences,Vol. XXXVIII, Part 5, (2010).
[10] Roncella R, Re C and Forlani G. “Comparison of two Structure and Motion Strategies”, Proc. 4th. ISPRS International Workshop 3D-ARCH: 3D Virtual Reconstruction and Visualization of Complex Architectures, Trento, Italy, 2-4 March 2011.
[11] Malzbender T and Ordentlich E.,”Maximum Entropy Lighting for Physical Objects”, Technical Report HPL-2005-68, Hewlett-Packard Laboratories Palo Alto. (2005)
[12] Besl, Paul J.; McKay, N.D., “A Method for Registration of 3-D Shapes”, IEEE Trans. on Pattern Analysis and Machine Intelligence (Los Alamitos, CA, USA: IEEE Computer Society) 14 (2): 239–256. (1992).
[13] Re C. Three dimensional reconstruction of planetary surfaces from stereo satellite images. (2014)